HHS Public Access

Author manuscript

J Cell Physiol. Author manuscript; available in PMC 2021 January 01.

Published in final edited form as:

J Cell Physiol. 2021 January ; 236(1): 664–676. doi:10.1002/jcp.29894.

Irisin deficiency disturbs bone metabolism

Xiaofang Zhu[1,2], **Xiangfen Li**[2], **Xiaoxuan Wang**[2], **Ting Chen**[2], **Fengjuan Tao**[2], **Chuanju Liu**[3], **Qisheng Tu**[2], **Guofang Shen**[1], **Jake J. Chen**[2,4]

[1]Department of Oral & Cranio-Maxillofacial Surgery, Shanghai Ninth People's Hospital, Shanghai Jiao Tong University School of Medicine, Shanghai Key Laboratory of Stomatology, Shanghai, China

[2]Division of Oral Biology, Tufts University School of Dental Medicine, Boston, Massachusetts

[3]Department of Orthopedics Surgery and Department of Cell Biology, New York University School of Medicine, New York, New York

[4]Department of Developmental, Molecular and Chemical Biology, Tufts University School of Medicine, Boston, Massachusetts

Abstract

Balancing the process of bone formation and resorption is important in the maintenance of healthy bone. Therefore, the discovery of novel factors that can regulate bone metabolism remains needed. Irisin is a newly identified hormone-like peptide. Recent studies have reported the involvement of irisin in many physiological and pathological conditions with bone mineral density changes, including osteopenia and osteoporotic fractures. In this study, we generated the first line of Osx-Cre:FNDC5/irisin KO mice, in which FNDC5/irisin was specifically deleted in the osteoblast lineage. Gene and protein expressions of irisin were remarkably decreased in bones but no significant differences in other tissues were observed in knockout mice. FNDC5/irisin deficient mice showed a lower bone density and significantly delayed bone development and mineralization from early-stage to adulthood. Our phenotypical analysis exhibited decreased osteoblast-related gene expression and increased osteoclast-related gene expression in bone tissues, and reduced adipose tissue browning due to bone-born irisin deletion. By harvesting and culturing MSCs from the knockout mice, we found that osteoblastogenesis was inhibited and osteoclastogenesis was increased. By using irisin stimulated wildtype primary cells as a gain-of-function model, we further revealed the effects and mechanisms of irisin on promoting osteogenesis and inhibiting osteoclastogenesis in vitro. In addition, positive effects of exercise, including bone strength enhancement and body weight loss were remarkably weakened due to irisin deficiency.

Correspondence Qisheng Tu and Jake J. Chen, Division of Oral Biology, Tufts University School of Dental Medicine, 136 Harrison Ave, M&V 811, Boston, MA 02111. qisheng.tu@tufts.edu (Q. T.) and jk.chen@tufts.edu (J. C.).

AUTHOR CONTRIBUTIONS

Conception and design, collection and assembly of data, data analysis and interpretation, manuscript writing: X. Z; provision of study material, collection and assembly of data: X. L. and X. W; data analysis and interpretation: T. C. and F. T; conception and design, financial support, data analysis and interpretation, manuscript writing: C. L., G. S., Q. T., and J. C; all authors approved the final version of the manuscript.

CONFLICT OF INTERESTS

The authors declare that there are no conflict of interests.

SUPPORTING INFORMATION

Additional supporting information may be found online in the Supporting Information section.

Interestingly, these changes can be rescued by supplemental administration of recombinant irisin during exercise. Our study indicates that irisin plays an important role in bone metabolism and the crosstalk between bone and adipose tissue. Irisin represents a potential molecule for the prevention and treatment of bone metabolic diseases.

Keywords

bone metabolism; bone mineralization; conditional knockout; irisin/FNDC5

1 | INTRODUCTION

Bone metabolism is a dynamic process of bone remodeling (Christenson, 1997). The biology of bone during mineral metabolism, especially the tightly coupled balance between bone formation by osteoblasts and bone resorption by osteoclasts, remains a challenge to clinical and basic science researchers (Seeman, 2009; Sims & Martin, 2014). Metabolic bone diseases (Demellawy, Davila, Shaw, & Nasr, 2018) caused by abnormalities of mineralization, including rickets (Wagner & Greer, 2008), osteoporosis (Aspray & Hill, 2019; Varacallo & Fox, 2014), and osteogenesis imperfecta (Demellawy et al., 2018), are among the most common chronic diseases affecting adults and children in industrialized countries. Approximately 10 million American men and women have osteoporosis, and more than one-half of the US population of 50 years and older has low bone density (Golob & Laya, 2015). Prevention and treatment of metabolic bone diseases are becoming increasingly important.

Irisin is a hormone-like peptide that is released on the cleavage of the membrane protein fibronectin-type III domain-containing 5 (FNDC5). This molecule was initially shown to participate in white adipose tissue (WAT) browning and energy expenditure (Boström et al., 2012). More recent studies have shown that irisin has multiple roles in many different tissues and organs including adipose tissue, nervous and skeletal systems. Irisin has appeared in many pathological processes as well, including inflammation and carcinogenesis (Korta, Pocheć, & Mazur-Biały, 2019; Mahgoub, D'Souza, Al Darmaki, Baniyas, & Adeghate, 2018; Polyzos et al., 2018). In the area of bone metabolism, irisin has been shown to be involved in many physiological and pathological conditions including bone mineral density (BMD) impairment in type II diabetes mellitus (T2DM; M. Zhang et al., 2014), renal disease (Ebert et al., 2014), osteopenia (Iemura, Kawao, Okumoto, Akagi, & Kaji, 2019), and osteoporotic fractures (Anastasilakis et al., 2014; Palermo et al., 2015; Yan, Liu, Guo, & Yang, 2018). These findings have not only shown the potential of irisin to be a biochemical marker of many bone mineral-related diseases but also led us to hypothesize that irisin might be directly involved in bone metabolism.

Our previous study showed increased circulating irisin levels during exercise in mice (J. Zhang, Valverde, et al., 2017), while other researchers have found similar findings in humans (Brenmoehl et al., 2014; Tsuchiya, Mizuno, & Goto, 2018). We also found that exercise induces high levels of both irisin messenger RNA (mRNA) and protein expression in murine bone tissues. Irisin increases both the number of osteoblast cells and the thickness

of trabecular and cortical bones in mice (J. Zhang, Valverde, et al., 2017). Despite these promising findings, a loss-of-function animal model is necessary to directly delineate the effect of irisin on bone metabolism.

This study was designed to establish an irisin bone-specific knockout mouse line and use it as a loss-of-function model to determine the effects of irisin deficiency during bone development, metabolism, and physical activity. Using a gene knockout strategy, and additional in vitro, in vivo, and ex vivo approaches including animal exercise and administration of exogenous irisin, we investigated how irisin deficiency disturbs bone metabolism, and the beneficial effects of irisin on bone health in mice.

2 | MATERIALS AND METHODS

2.1 | Generation of knockout mice in which irisin expression is specifically deleted in osteogenic lineage

Using the transgenic Cre-loxP system, a targeting strategy was designed. After scanning the gene structure and the size of exons, we determined that exon 2 of FNDC5 could be conditionally removed and will result in a 75 aa (28 aa N-terminal sequence of irisin and 47 aa frame-shifted nonsense aa) truncation. With this strategy, the FNDC5/irisin$^{flox/flox}$ mice of C57BL/6J background carrying the FNDC5/irisin gene bordered with two loxP sequences, were constructed. We then mated the FNDC5/irisin$^{flox/flox}$ mice with the osterix (Sp7 or Osx)-Cre mice (006361; Jackson Laboratory), the transgenic mice expressing the Cre recombinase gene under the control of the SP7 promoter. The Osx-Cre: FNDC5/Irisin$^{flox/-}$ offspring were used to generate the Osx-Cre: FNDC5/Irisin KO mice. The Osx-Cre: FNDC5/Irisin$^{-/-}$ mice from the same litter were used as controls. For conciseness, we will use the abbreviation of F/I KO to represent “Osx-Cre:FNDC5/Irisin KO mice” in the remainder of this paper. All mice used in this study were housed at the Tufts Medical Center Animal Facility (Boston, MA), which is fully accredited by the American Association for Accreditation of Laboratory Animal Care. The Institutional Animal Care and Use Committee (IACUC) approved the animal protocols for this study. Mice were maintained under standardized conditions as described previously (L. Zhang, Tang, et al., 2017).

2.2 | DNA extraction and genotyping

The tail DNA samples were extracted from 2-week-old and postnatal day 2 pups offspring of F/I KO mice, respectively, following instructions from the DNeasy® Blood & Tissue Kit (Qiagen; Cat no. 69506). Southern blot was performed on the ES cells and the F2 generation of the KO mice as previously described (Dubeau, Chandler, Gralow, Nichols, & Jones, 1986), while standard polymerase chain reaction (PCR) was performed on all generated mice (L. Zhang, Tang, et al., 2017). The primer sequences are provided in Table S1. Mice were grouped based on the genotyping results.

2.3 | Tissue sampling and enzyme-linked immunosorbent assay (ELISA) for irisin

The tissues of femur, tibia, skeletal muscle, and subcutaneous WAT were collected for mRNA and protein analyses and stored at −80°C till use. Serum samples were collected as previously described (J. Zhang, Valverde, et al., 2017 2017). In brief, the blood was obtained

using cardiac puncture, then the serum was isolated by centrifugation and stored at −80°C. Peripheral circulating irisin levels were analyzed and quantified with an ELISA Kit (Phoenix Pharmaceuticals, Inc.) following the manufacturer's recommendations.

2.4 | Analysis of gene and protein expression

Total RNA of tissues and cells was isolated using TRIzol (Thermo Fisher Scientific) and the Quick-RNATM MiniPrep Kit (Zymo, CA). RNA of each sample was reverse-transcribed by M-MLV Reverse Transcriptase (Promega, WI) and cDNAs were quantified by real-time PCR with SYBR Green Supermix (Affymetrix) on Bio-Rad iQ5 (Bio-Rad Laboratories, CA). The primer sequences used are listed in Table S2.

The protein of the femurs, tibias, and skeletal muscles, and bone marrow–derived mesenchymal cells (BMSCs) and bone marrow–derived macrophage (BMM) cells, were extracted as previously described (J. Zhang, Valverde, et al., 2017). Whole protein samples were extracted using the RIPA lysis buffer (Santa Cruz Biotechnology Inc., TX). The nuclear and cytoplasm proteins were separated by a nuclear extraction kit (EMD Millipore, Germany) followed by sodium dodecyl sulfate-polyacrylamide gel electrophoresis and western blot analyses. Antibodies for β-catenin (1:2,000), β-actin (1:1,000), P-AKT1 (1:1,000), P-p38 (1:1,000), AKT1 (1:1,000), p38 (1:1,000) and calcineurin (1:1,000) were purchased from Cell Signaling Technology and the antibodies for nuclear factor of activated T cells c1 (Nfatc1; 1:1,000) and lamin B1 (1:1,000) were from Santa Cruz Biotechnology. Irisin pAb (IN102; AG-25B-0027) antibody (1:1,000) to detect irisin and FNDC5 expression was purchased from AdipoGen Corporation.

2.5 | Microcomputed tomography (μCT) analysis

The mice (n = 5 per group) were anesthetized by isoflurane inhalation (1.5–2.0%) and scanned using a live animal microcomputed tomography (μCT) system (SkyScan1172; Bruker-microCT, Belgium) at Tufts Medical Center. The 3D models were then reconstructed from the raw images with Bruker NRecon and analyzed with software from Bruker, including CT Analyser 1.17.7.2, DataViewer 1.5.4.0 and CT Vox 3.3.0. The morphometric indices, including Co.BS/BV, Tb.BV/TV, BMD, and Tb.Sp were calculated (Bouxsein et al., 2010).

2.6 | Primary cell isolation and culture for analytical studies

2.6.1 | Isolation and osteogenesis induction of BMSCs—

Six-week-old C57BL/6J mice (000664; Jackson Laboratory), FNDC5/irisin$^{flox/flox}$ mice and Osx-Cre:FNDC5/Irisin KO mice were first killed by cervical dislocation following anesthesia respectively. The mice were sterilized with 70% (vol/vol) ethanol. The hind legs were removed from the body using scissors and all skin and muscle tissues were removed from the legs. The epiphyses of femur and tibia were cut off. The bone marrow was flushed out with Dulbecco's modified Eagle's medium (DMEM; Gibco® by Life Technologies™) from the long bones, then cultured in the DMEM with 10% fetal bovine serum (FBS) in a 5% CO_2 incubator, at 37°C. After 3 hr, nonadherent cells were carefully removed and fresh medium was added. The BMSCs were treated with osteoblast differentiation medium (DM) including ascorbic acid (Asc, 50 μg/ml), dexamethasone (Dex, 0.1 μM) and β-

glycerophosphate (β-Gly, 10 mM) with or without of irisin (4 and 20 μmol/L) for 5, 7, 14, and 21 days followed by RNA isolation. For protein extraction, we serum-starved the BMSCs overnight and then treated them with DM in the presence or absence of irisin for 1, 2, 3, and 6 hr.

2.6.2 | Isolation and osteoclastogenesis induction of BMM cells—Bone marrow cells were harvested as aforementioned and then treated as previously described (Qu et al., 2014; Weischenfeldt & Porse, 2008; Zhai et al., 2014). In brief, the cells were vigorously pipetted to disintegrate the cells into a single-cell suspension, and then incubated in RPMI 1640 (Gibco® by Life Technologies™) with 10% FBS and M-CSF (10 ng/ml, Pepro Tech, Inc.). The cells were washed with phosphate-buffered saline (PBS) three times every other day, and macrophage progenitors which adhered to the cell dish remained. The BMMs were harvested on Day 7 and then plated and incubated for another 24 hr. The BMMs were treated with 10 ng/ml M-CSF plus 50 ng/ml receptor activator of receptor activator of nuclear factor-κB ligand (RANKL) in the presence or absence of irisin (4 and 20 μmol/L) for 3–5 days. To determine the protein phosphorylation levels, the BMMs were serum-starvation treated overnight and then stimulated for 10, 30, and 60 min.

2.7 | Cell staining and histomorphological staining

2.7.1 | Alizarin red staining—Alizarin red S (ARS; Sigma-Aldrich; A-5533) 40 mM dissolved in 100 ml PBS. Adjusted the pH to 4.2. Cells were washed with PBS, then fixed with 10% formalin for 5 min and rinsed again with dH_2O. We carefully aspirated dH_2O and added alizarin red solution to cover the cells and incubated at room temperature for 10 min followed by dH_2O rinse. The alizarin red stained mineralized nodules were then melted with 10% (vol/vol) cetylpyridinium chloride. The absorbance at 562 nm by the dissolved alizarin red stain was measured to quantify the alizarin red stain as we and others previously described. (Chen, Wu, Wang, & Li, 2014; Tang et al., 2018).

2.7.2 | Tartrate-resistant acid phosphatase (TRAP) staining of osteoclasts—A leukocyte acid phosphatase TRAP Kit from Sigma-Aldrich was used for TRAP staining in osteoclasts following the manufacturer's recommended protocol.

2.7.3 | Alkaline phosphatase staining—The cells were prepared the same as described in the alizarin red staining methods. The BCIP®/NBT Liquid Substrate System (Sigma-Aldrich) was used for determining alkaline phosphatase activity, which is essential for normal mineralization, in osteoblasts.

2.7.4 | Hemotoxylin and eosin (H&E) staining and TRAP staining of bone tissue—The left proximal tibia of F/I KO and control mice were fixed in 4% Paraformaldehyde, embedded with paraffin, and cut into 5 μm sections. H&E staining and TRAP staining were performed according to the manufacturer's instructions. Digital images were taken with a OLYMPUS BX53 microscope (Olympus, Waltham, MA).

2.7.5 | Alcian blue/alizarin red staining of cartilage and bone in mouse—Postnatal day 2 pups ($n = 3$ per group) were processed for whole skeleton staining with

alcian blue (cartilage) and alizarin red (bone) following standard procedures as previously described (Rigueur & Lyons, 2014; Tu et al., 2003).

2.8 | Voluntary wheel running exercise and the rescue of irisin deficiency

We conducted a 14-day voluntary wheel running experiment on the F/I KO mice and control mice, and setup a third group of F/I KO mice with daily r-irisin injection to examine the effects of loss and gain function of irisin in physical activities. We setup a baseline of average 2,000 revolutions per day and only animals with counts over the baseline are included in the analysis (n = 5–6 per group). The resultant average counts per day for the control, KO mice and KO mice + irisin injection group are: 7,599.8, 6,830.6, and 7,002.2, respectively. No significant difference in running counts was observed among the three groups. To eliminate the impact of base body weight from different groups, we evaluated body weight percentage loss instead of body weight absolute loss.

2.9 | Statistical analysis

All data are presented as means ± SD of results obtained from three or more experiments. The significance of differences in various categorical variables was evaluated using one-way analysis of variance for multi-group comparisons and the t test for between two group comparisons. A p value of less than .05 was considered to be statistically significant. All statistical analyses were performed using SPSS statistics 18.0 (SPSS Inc., IL) and Prism GraphPad 6.0 (GraphPad Software).

3 | RESULTS

3.1 | Generation and identification of F/I KO mice

The designed F/I KO mice (Figure 1a) were genotyped by southern blot and standard PCR (Figure 1b). Homozygous KO mice were achieved in the third generation. The mRNA and protein expression levels of irisin were found to decrease in bone tissues of the F/I KO mice compared with the control group, while no difference was observed in WAT and muscle (Figure 1c,d). These results indicate successful specific deletion of irisin in bone tissue of F/I KO mice.

3.2 | Bone development and mineralization in F/I KO mice

To investigate the effects of irisin deficiency on bone, whole skeleton staining was applied. Hypomineralization and immature bone matrix were observed in the F/I KO group on postnatal day 2 (P2). The endochondral ossification of epiphysis of the limbs and the phalanges were significantly delayed. In contrast, the Alcian blue staining of cartilage was strongly positive in the ossification centers in the F/I KO mice (Figure 2a).

We next assessed the cellular basis for the bone phenotype in F/I KO mice. Histomorphological staining showed significant decrease in trabecular bone mass of proximal tibia in 2- and 4-week-old F/I KO mice (Figure 2b,A). Quantification of the trabecular area in H&E and TRAP staining sections showed a remarkable decrease in trabecular bone area (Trab.Ar.%) and osteoblast number per bone perimeter (Ob.N/B.Pm),

and a significant increase in osteoclast number per bone perimeter (Oc.N/B.Pm; Figure 2b,B).

The entire skeletal system of the F/I KO mice and the control mice were scanned and analyzed with live small animals μCT. The bone development and mineralization were found to be significantly delayed in F/I KO mice at 6, 10, and 18 weeks. Representative reconstruction images captured from different parts of the skeleton, including the skull, hyoid, ribs, xiphoid, and coccyx are shown in Figure 2c. Both the cortical bone mineral density (Co.BMD) and trabecular bone-to-tissue volume ratio (Tb.BV/TV) in femurs in the F/I KO group were found to be considerably lower than those in the control group, while the cortical bone surface-to-volume ratio (Co.BS/BV) was increased, indicating thinner cortical bone (Figure 2d).

3.3 | Bone-born irisin deletion affects circulating irisin and adipocytes browning in mice

The ELISA test exhibited lower serum irisin levels in the F/I KO group compared with the control group (Figure 1h). This result indicates the effects of FNDC5/irisin deletion in bone are not limited to the skeletal system. Real-time quantitative reverse-transcription PCR (qRT-PCR) showed a significantly lower expression level of browning related gene markers in WAT, including Cidea, PR domain-containing 16 (Prdm16), and uncoupling protein 1 (Ucp-1) in the F/I KO mice than in the control mice (Figure 1g).

3.4 | Osteogenic gene expression in F/I KO mice

In the femurs of the F/I KO mice, the relative mRNA level expression of osteogenic markers, collagen 1, bone sialoprotein (Bsp), and Osx, decreased (Figure 1e) while the osteoclastogenesis-related gene marker matrix metalloproteinase 9 (Mmp9) increased (Figure 1f).

The effects of endogenous irisin defect on osteoblast differentiation were analyzed in vitro by harvesting and culturing the BMSCs from both the F/I KO and control mice. With the same osteoblast induction, the F/I KO group showed reduced osteoblast differentiation. The osteogenic markers, including collagen 1, Runt-related transcription factor 2 (Runx2), Bsp, Osx, and alkaline phosphatase (Alp) remarkably decreased on both Day 5 and Day 7 (Figure 3a). The precipitation of ALP staining, which marks hypertrophic cells before mineralization onset (McComb, Jr, & Posen, 2013), decreased in the F/I KO group (Figure 3b). ARS staining showed calcium-rich deposits in cells and indicates the formation of bone nodules (Gregory, Gunn, Peister, & Prockop, 2004). The ARS staining and the concentration of the melted nodules solution, was also significantly lower in the F/I KO group on days 14 and 21 (Figure 3c).

By harvesting and induced-culturing the BMMs from the F/I KO and control mice, we observed that the mRNA expression level of osteoclastogenesis markers, including cathepsin K, Mmp9, and Trap, increased on Day 4 (Figure 3d). The TRAP staining, which is commonly used to identify osteoclasts, showed the number of TRAP + osteoclast cells were increased in the KO group on Day 4 (Figure 3e).

3.5 | Effects of irisin on osteoblast differentiation, bone formation and mineralization in BMSCs

The direct effects of exogenous irisin on osteoblast differentiation were evaluated on the BMSCs. The qRT-PCR analysis revealed that the irisin promoted the osteogenic differentiation of BMSCs by upregulating the mRNA expression of several osteogenic markers, including Runx2, special AT-rich sequence-binding protein 2, Bsp, collagen I, and Alp after 5 days treatment with recombinant irisin (r-irisin; Figure 4a). Western blot results showed significantly higher total β-catenin protein level in the BMSCs treated with r-irisin at 1 hr (Figure 4b). The cytoplasmic β-catenin level gradually and slightly decreased during the 6-hr period of irisin treatment (Figure 4c). The levels of nuclear β-catenin significantly increased, especially in the 3- and 6-hr groups (Figure 4d). These dynamic changes of the β-catenin protein level are due to its accumulation and nuclear translocation, which is a key factor in activating the Wnt/β-catenin pathway. We also analyzed the mineralization of BMSCs in the presence or absence of irisin. A higher ARS staining level was found in both low- and high-dose irisin-treated groups than the osteoblast induction only group at 3 weeks. The concentration of the melted nodules solution showed consistent results (Figure 4e).

3.6 | Irisin inhibits RANKL-induced osteoclastogenesis in BMMs

Next, we evaluated the ability of irisin to directly inhibit RANKL-induced osteoclast differentiation of the primary macrophage cells in vitro. In the presence of irisin, the mRNA expression level of osteoclastogenesis markers, including Trap, Mmp9, and Nfatc1, was markedly decreased, especially in the high-dose irisin group (Figure 4f). We then measured the Nfatc1 protein expression level and found high-dose irisin treatment (20 nM) decreased the RANKL upregulation of Nfatc1 significantly (Figure 4g). Additional western blot analyses determined the protein level of p-Akt1, Akt1, p-p38, p38, and calcineurin in the BMMs cultures treated with and without irisin for 0, 10, 30 and 60 min. The phosphorylation of Akt1 was significantly suppressed with irisin treatment (Figure 4h). TRAP staining and TRAP-positive multinucleated cells ($TRAP^+$ MNCs, more than three nuclei) counting showed reduced $TRAP^+$ MNCs number by approximately one-half in the RANKL + irisin treatment groups compared to the RANKL-induced only group on Day 5 (Figure 4i). Our results indicate that the irisin impaired the RANKL-induced AKT cascade and suppressed the activation of NFATc1 of osteoclast differentiation.

3.7 | Wheel running exercise and F/I KO mice rescue with exogenous irisin compensation

As lower browning related gene marker levels in the KO group were shown (Figure 1g), we speculated that exercise-induced white adipose tissue browning might also be affected by bone-born irisin deficiency. To verify this hypothesis, an experiment of 14-day voluntary wheel running was performed. μCT analysis showed significant intragroup changes of cortical bone thickness in both the Control group and F/I KO + irisin injection group, but these were insignificant in the F/I KO group (Figure 5a,d). On the other hand, the body weight percentage loss of the control group, KO group, and KO + inj groups were 17%, 5%, and 14%, respectively (Figure 5b). The serum irisin level of the KO group was significantly lower than that of the control group while that in the KO + inj group was significantly higher than the control group after 14 days of irisin injection (Figure 5c). The expression of adipose

tissue browning related genes, including Prdm16, Cidea, peroxisome proliferator-activated receptor-γ coactivator 1α (Pgc-1α), in subcutaneous fat was also found to be lower in the KO group but higher in the KO + inj group compared with the control group (Figure 5e).

4 | DISCUSSION

We investigated the effects of irisin in modulating bone metabolism from multiple perspectives. In our in vitro studies of the BMSCs, ALP and alizarin red staining revealed increased mineralization in r-irisin-treated wildtype BMSCs and decreased mineralization in irisin deficiency BMSCs. In vivo, the whole skeleton staining of bone-born irisin deficient mice showed more blue-stained cartilage matrix at the epiphyses and the immature bone matrix on postnatal Day 2. Histomorphological staining showed a lower trabecular area percentage, decreased osteoblast number and increased osteoclast number when normalized to bone perimeter in 2- and 4-week-old F/I KO mice. The μCT analysis demonstrated a continuous hypomineralization phenotype in bone formation from Week 6 to Week 18, and the measurement of BMD and BV/TV presented persistent lower bone density in F/I KO mice. These indicate bone-born irisin deficiency significantly disturbed skeletal development and mineralization. Interestingly, we also observed high expression of irisin in cartilage on E17.5 by immunohistochemistry (IHC; Figure S3). The effects of irisin on cartilage and endochondral ossification will be further investigated in our ongoing work.

We studied the primary cells from the F/I KO mice, a loss-of-function model ex vivo. We observed decreased osteoblastogenesis and enhanced osteoclastogenesis in primary cells from knockout mice. This indicates the endogenous osteoblast-secreted irisin may be a paracrine factor for osteoclast lineage in addition to its autocrine effects on osteoblasts. Conversely, to setup a matched gain-of-function model of irisin for mechanistic study, we stimulated the primary cells, the BMSCs and the BMMs, from wildtype mice with exogenous r-irisin. We proved that irisin increases osteoblastogenesis and inhibits osteoclastogenesis, which is consistent with the previous studies in cell lines from our lab (J. Zhang, Valverde, et al., 2017) and other researchers (Colaianni et al., 2014; Qiao et al., 2016). These results together with other studies revealed that both exogenous and endogenous irisin have significant effects on the bone remodeling process. The dynamic changes of β-catenin protein level indicate that irisin increases osteoblastogenesis through the Wnt/β-catenin pathway. The Akt/GSK3β/NFATc1 signaling axis plays an important role in RANKL-induced osteoclastogenesis (Moon et al., 2012). In our study, irisin impaired RANKL-induced AKT activation and suppressed RANKL-induced activation of NFATc1. Further study on the exact molecular signals irisin directly triggered that regulate the balance between bone resorption and formation are needed and meaningful.

Previous studies demonstrated the function of exogenous r-irisin and muscle secreted irisin in adipose tissue browning, inducing weight loss via the PGC-1α/Irisin/UCP-1 pathway during exercise (Boström et al., 2012; Dinas et al., 2017; Niranjan, Belwalkar, Tambe, Venkataraman, & Mookhtiar, 2019; J. Zhang, Valverde, et al., 2017). In our study, we surprisingly found a marked decrease in the levels of the gene markers related to adipose tissue browning in bone-specific FNDC5/irisin deficient mice. Furthermore, we performed a wheel running exercise with and without r-irisin daily injection for 2 weeks on the F/I KO

mice. In this study, for the first time, we found that the lack of bone-born irisin can significantly weaken the weight loss induced by exercise. And this phenomenon can be rescued by r-irisin compensation during the exercise. In addition, the browning gene markers expression significantly increased in the rescue group. A recent report about Osx-Cre targeting multiple types of cells including adipocytes may partly explain these phenomena (Chen et al., 2014). In addition, the lower circulating irisin level may also contribute to the adipose tissue phenotypes of the F/I KO mice. Moreover, it gives us new insights into understanding the effects of irisin in the crosstalk among bone, muscle and adipose tissue. We hypothesized that bone-secreted irisin may be a endocrine or local paracrine factor for adipocytes as a messenger between bone and adipose tissues. There are already hundreds of clinical and preclinical studies about the effects of systemic irisin in various disease states. But there has not been any comprehensive study on the autocrine, paracrine and endocrine effects of irisin.

We used the Cre-loxP system to create conditional knockout mice. After scanning the gene structure and the size of exons, we found the introns flanks exon 2 are 1,527 and 536 bp—large enough to insert the loxP elements. Hence, we inserted the loxP sequences to the introns on both ends of the exon 2. Additionally, there were no significant regulatory elements, so the insertion of loxP elements will not interfere with mRNA splicing and native irisin expression. Osx-Cre mouse has been widely used in the bone research field, it has both tTA and tetracycline (Tet)-Off regulatable GFP/Cre fusion protein expression under the control of the Osterix promoter (Rodda & McMahon, 2006; Wang, Mishina, & Liu, 2015). The Osx-Cre null littermates are commonly used as the control group (Li et al., 2017; Razidlo et al., 2010). However, recent studies found minor or severe defects on craniofacial and cortical bone caused by Osx-Cre itself during the early postnatal stage (Davey et al., 2012; Razidlo et al., 2010; Wang et al., 2015). Therefore, to avoid the impact of Osx-Cre expression on the results, we carefully chose Cre-positive littermates as the control. In addition, it was also demonstrated that Osx-Cre mice have no effect on the trabecular bone, and the craniofacial and cortical bone defects gradually recovered during development and largely disappeared by 3 weeks of age (Davey et al., 2012; F. Liu et al., 2013; Y. Liu et al., 2012). In our experiments, however, certain trabecular bone changes in the F/I KO mice were observed, and our data has a timespan across months from postnatal stage to fully grown adult mice. Considering all these factors, our evaluation and analysis of the F/I KO mice were not affected by the Osx-Cre mediated deletion. On the other hand, the effect of lacking irisin in other systems in vivo, such as adipose metabolism and nervous system is still unknown. Our $F/I^{flox/flox}$ mice are ready for use in any further study on other tissues.

Our data and a majority of studies have demonstrated a positive correlation between irisin and healthy bone anabolism in both humans (Al-Daghri et al., 2016; Anastasilakis et al., 2014; Fawzy, Elghaffar, Mahmoud, & Helmy, 2018; Gallagher & Tella, 2014; Hamann, Kirschner, Günther, & Hofbauer, 2012; Klangjareonchai et al., 2014; Palermo et al., 2015; Park, Kim, Zhang, Yeom, & Lim, 2018; Serbest, Tiftikçi, Tosun, & Kisa, 2017; Singhal et al., 2014; Wu et al., 2018; Yan et al., 2018), and mice (Colaianni et al., 2017; Grano et al., United States Patent No. US20180153960A1, 2018; Metzger, Narayanan, Zawieja, & Bloomfield, 2018; Narayanan, Metzger, Bloomfield, & Zawieja, 2018), and in vitro studies (Colaianni et al., 2014, 2015; Kawao, Moritake, Tatsumi, & Kaji, 2018; Ma et al., 2018;

Qiao et al., 2016; D. Zhang et al., 2018; J. Zhang, Valverde, et al., 2017). A recently published study showed a negative relationship between these two (Kim et al., 2018). Their results suggested that irisin increases sclerostin expression in osteocytes and further induces bone resorption. Genetic deletion of FNDC5/irisin completely blocked OVX-induced trabecular bone loss in their study. However, the results from other groupsm including ours, are the opposite. Independent research teams reported that in osteocyte-like MLO-Y4 cells, r-irisin significantly downregulates scleorostin (Sost; D. Zhang et al., 2018), and irisin inhibits osteoclast differentiation (Kawao et al., 2018; Ma et al., 2018; J. Zhang, Valverde, et al., 2017). According to Colainni's in vivo study, low doses r-irisin injection on young male mice decreases the expression of osteoblastic inhibitory genes such as Sost in tibiae (Colaianni et al., 2015). Furthermore, irisin treatment was reported to prevent the loss of bone mass in ovariectomized mice (Grano et al., United States Patent No. US20180153960A1, 2018). Among clinical studies, a large population study shows the positive correlation between plasma irisin and BMD (Wu et al., 2018). In polycystic ovary syndrome patients, the circulating irisin level and BMD have a strong positive correlation (Fawzy et al., 2018). Low concentrations of circulating irisin are associated with increased risk of osteoporotic fracture, especially in postmenopausal women (Anastasilakis et al., 2014; Gallagher & Tella, 2014; Palermo et al., 2015; Park et al., 2018; Yan et al., 2018; Zhou, Qiao, Cai, Li, & Shan, 2019). Sclerostin and irisin are negatively correlated in both males and females (Klangjareonchai et al., 2014). The level of irisin hormone increased in the bone union process and affects fracture healing (Serbest et al., 2017). We conclude that irisin has a protective role in bone health.

Irisin, as a multifunctional protein, and has implications on health and many diseases (Korta et al., 2019). Our study showed that irisin plays an important role in bone metabolism and the crosstalk between bone and adipose tissue. Irisin represents a potential molecule for the prevention and treatment of bone metabolic diseases. The broader effects of irisin will be further investigated in our ongoing work.

Supplementary Material

Refer to Web version on PubMed Central for supplementary material.

ACKNOWLEDGMENTS

This study was supported by the National Institutes of Health (NIH) grants AR62207 to C. L.; R01 DE21464, R01 DE25681, and R01 DE26507 to J. C.

Funding information

National Institutes of Health, Grant/Award Numbers: AR62207, R01 DE21464, R01 DE25681, R01 DE26507

DATA AVAILABILITY STATEMENT

The data that support the findings of this study are available from the corresponding author upon reasonable request.

REFERENCES

Al-Daghri NM, Rahman S, Sabico S, Amer OE, Wani K, Al-Attas OS, & Alokail MS (2016). Impact of vitamin D correction on circulating irisin: A 12 month interventional study. International Journal of Clinical and Experimental Medicine, 9(7), 13086–13092.

Anastasilakis A, Polyzos S, Makras P, Gkiomisi A, Bisbinas I, Katsarou A, … Mantzoros C (2014). Circulating irisin is associated with osteoporotic fractures in postmenopausal women with low bone mass but is not affected by either teriparatide or denosumab treatment for 3 months. Osteoporosis International, 25(5), 1633–1642. 10.1007/s00198-014-2673-x [PubMed: 24599275]

Aspray TJ, & Hill TR (2019). Osteoporosis and the ageing skeleton In Harris JR & Korolchuk VI (Eds.), Biochemistry and cell biology of ageing: Part II. Clinical science (pp. 453–476). Berlin: Springer 10.1007/978-981-13-3681-2_16

Boström P, Wu J, Jedrychowski M, Korde A, Ye L, Lo J, … Spiegelman B (2012). A PGC1-α-dependent myokine that drives brown-fat-like development of white fat and thermogenesis. Nature, 481(7382), 463–468. 10.1038/nature10777 [PubMed: 22237023]

Bouxsein ML, Boyd SK, Christiansen BA, Guldberg RE, Jepsen KJ, & Müller R (2010). Guidelines for assessment of bone microstructure in rodents using micro-computed tomography. Journal of Bone and Mineral Research, 25(7), 1468–1486. 10.1002/jbmr.141 [PubMed: 20533309]

Brenmoehl J, Albrecht E, Komolka K, Schering L, Langhammer M, Hoeflich A, & Maak S (2014). Irisin is elevated in skeletal muscle and serum of mice immediately after acute exercise. International Journal of Biological Sciences, 10(3), 338–349. 10.7150/ijbs.7972 [PubMed: 24644429]

Chen J, Shi Y, Regan J, Karuppaiah K, Ornitz DM, & Long F (2014). Osx-Cre targets multiple cell types besides osteoblast lineage in postnatal mice. PLOS One, 9(1), e85161 10.1371/journal.pone.0085161 [PubMed: 24454809]

Chen SH, Wu C-C, Wang S-H, & Li WT (2014). Growth and differentiation of osteoblasts regulated by low-intensity pulsed ultrasound of various exposure durations. Journal of Medical and Biological Engineering, 34(2), 197–203. 10.5405/jmbe.1346

Christenson RH (1997). Biochemical markers of bone metabolism: An overview. Clinical Biochemistry, 30(8), 573–593. 10.1016/S0009-9120(97)00113-6 [PubMed: 9455610]

Colaianni G, Cuscito C, Mongelli T, Oranger A, Mori G, Brunetti G, … Grano M (2014). Irisin enhances osteoblast differentiation in vitro. International Journal of Endocrinology, 2014, 902186 10.1155/2014/902186 [PubMed: 24723951]

Colaianni G, Cuscito C, Mongelli T, Pignataro P, Buccoliero C, Liu P, … Grano M (2015). The myokine irisin increases cortical bone mass. Proceedings of the National Academy of Sciences, 112(39), 12157–12162. 10.1073/pnas.1516622112

Colaianni G, Mongelli T, Cuscito C, Pignataro P, Lippo L, Spiro G, … Grano M (2017). Irisin prevents and restores bone loss and muscle atrophy in hind-limb suspended mice. Scientific Reports, 7, 2811 10.1038/s41598-017-02557-8 [PubMed: 28588307]

Davey RA, Clarke MV, Sastra S, Skinner JP, Chiang C, Anderson PH, & Zajac JD (2012). Decreased body weight in young Osterix-Cre transgenic mice results in delayed cortical bone expansion and accrual. Transgenic Research, 21(4), 885–893. 10.1007/s11248-011-9581-z [PubMed: 22160436]

Demellawy D, Davila J, Shaw A, & Nasr Y (2018). Brief review on metabolic bone disease. Academic Forensic Pathology, 8(3), 611–640. 10.1177/1925362118797737 [PubMed: 31240061]

Dinas PC, Lahart IM, Timmons JA, Svensson P-A, Koutedakis Y, Flouris AD, & Metsios GS (2017). Effects of physical activity on the link between PGC-1a and FNDC5 in muscle, circulating Irisin and UCP1 of white adipocytes in humans: A systematic review. F1000Research, 6, 286 10.12688/f1000research.11107.2 [PubMed: 28620456]

Dubeau L, Chandler LA, Gralow JR, Nichols PW, & Jones PA (1986). Southern blot analysis of DNA extracted from formalin-fixed pathology specimens. Cancer Research, 46(6), 2964–2969. [PubMed: 3009004]

Ebert T, Focke D, Petroff D, Wurst U, Richter J, Bachmann A, … Fasshauer M (2014). Serum levels of the myokine irisin in relation to metabolic and renal function. European Journal of Endocrinology, 170(4), 501–506. 10.1530/EJE-13-1053 [PubMed: 24399249]

Fawzy O, Elghaffar NA, Mahmoud E, & Helmy A (2018). Bone mineral density in relation to polycystic ovary syndrome: An insight into irisin and insulin. The Scientific Journal of Al-Azhar Medical Faculty, Girls, 2(3), 194 10.4103/sjamf.sjamf_35_18

Gallagher JC, & Tella SH (2014). Prevention and treatment of postmenopausal osteoporosis. The Journal of Steroid Biochemistry and Molecular Biology, 142, 155–170. 10.1016/j.jsbmb.2013.09.008 [PubMed: 24176761]

Golob AL, & Laya MB (2015). Osteoporosis: Screening, prevention, and management. The. Medical Clinics of North America, 99(3), 587–606. 10.1016/j.mcna.2015.01.010 [PubMed: 25841602]

Grano M, Colaianni G, Cuscito C, Brunetti G, Colucci S, Cinti S, & Mori G (2018). United States Patent No. US20180153960A1 Retrieved from https://patents.google.com/patent/US20180153960A1/en

Gregory CA, Gunn WG, Peister A, & Prockop DJ (2004). An Alizarin red-based assay of mineralization by adherent cells in culture: Comparison with cetylpyridinium chloride extraction. Analytical Biochemistry, 329(1), 77–84. 10.1016/j.ab.2004.02.002 [PubMed: 15136169]

Hamann C, Kirschner S, Günther K-P, & Hofbauer LC (2012). Bone, sweet bone—Osteoporotic fractures in diabetes mellitus. Nature Reviews Endocrinology, 8(5), 297–305. 10.1038/nrendo.2011.233

Iemura S, Kawao N, Okumoto K, Akagi M, & Kaji H (2019). Role of irisin in androgen-deficient muscle wasting and osteopenia in mice. Journal of Bone and Mineral Metabolism, 10.1007/s00774-019-01043-7

Kawao N, Moritake A, Tatsumi K, & Kaji H (2018). Roles of Irisin in the linkage from muscle to bone during mechanical unloading in mice. Calcified Tissue International, 103(1), 24–34. 10.1007/s00223-018-0387-3 [PubMed: 29332162]

Kim H, Wrann CD, Jedrychowski M, Vidoni S, Kitase Y, Nagano K, … Spiegelman BM (2018). Irisin mediates effects on bone and fat via αV integrin receptors. Cell, 175(7), 1756–1768.e17. 10.1016/j.cell.2018.10.025 [PubMed: 30550785]

Klangjareonchai T, Nimitphong H, Saetung S, Bhirommuang N, Samittarucksa R, Chanprasertyothin S, … Ongphiphadhanakul B (2014). Circulating sclerostin and irisin are related and interact with gender to influence adiposity in adults with prediabetes [Research article]. 10.1155/2014/261545

Korta P, Pocheć E, & Mazur-Biały A (2019). Irisin as a multifunctional protein: Implications for health and certain diseases. Medicina, 55(8), 10.3390/medicina55080485

Li S, Xu W, Xing Z, Qian J, Chen L, Gu R, … Deng F (2017). A conditional knockout mouse model reveals a critical role of PKD1 in osteoblast differentiation and bone development. Scientific Reports, 7, 40505 10.1038/srep40505 [PubMed: 28084409]

Liu F, Fang F, Yuan H, Yang D, Chen Y, Williams L, … Guan J-L (2013). Suppression of autophagy by FIP200 deletion leads to osteopenia in mice through the inhibition of osteoblast terminal differentiation. Journal of Bone and Mineral Research, 28(11), 2414–2430. 10.1002/jbmr.1971 [PubMed: 23633228]

Liu Y, Berendsen AD, Jia S, Lotinun S, Baron R, Ferrara N, & Olsen BR (2012). Intracellular VEGF regulates the balance between osteoblast and adipocyte differentiation. The Journal of Clinical Investigation, 122(9), 3101–3113. 10.1172/JCI61209 [PubMed: 22886301]

Ma Y, Qiao X, Zeng R, Cheng R, Zhang J, Luo Y, … Xu L (2018). Irisin promotes proliferation but inhibits differentiation in osteoclast precursor cells. The FASEB Journal, 32(11), 5813–5823. 10.1096/fj.201700983RR

Mahgoub MO, D'Souza C, Al Darmaki RSMH, Baniyas MMYH, & Adeghate E (2018). An update on the role of irisin in the regulation of endocrine and metabolic functions. Peptides, 104, 15–23. 10.1016/j.peptides.2018.03.018 [PubMed: 29608940]

McComb RB, Jr GNB, & Posen S (2013). Alkaline phosphatase. Springer Science & Business Media.

Metzger CE, Narayanan SA, Zawieja DC, & Bloomfield SA (2018). P035 Exogenous administration of irisin during chronic tnbs-induced gut inflammation reverses inflammation-induced alterations in bone turnover. Gastroenterology, 154(1, Suppl.), S18 10.1053/j.gastro.2017.11.072

Moon JB, Kim JH, Kim K, Youn BU, Ko A, Lee SY, & Kim N (2012). Akt Induces Osteoclast differentiation through regulating the GSK3β/NFATc1 signaling cascade. The Journal of Immunology, 188(1), 163–169. 10.4049/jimmunol.1101254 [PubMed: 22131333]

Narayanan SA, Metzger CE, Bloomfield SA, & Zawieja DC (2018). Inflammation-induced lymphatic architecture and bone turnover changes are ameliorated by irisin treatment in chronic inflammatory bowel disease. The FASEB Journal, 32(9), 4848–4861. 10.1096/fj.201800178R [PubMed: 29596023]

Niranjan SB, Belwalkar SV, Tambe S, Venkataraman K, & Mookhtiar KA (2019). Recombinant irisin induces weight loss in high fat DIO mice through increase in energy consumption and thermogenesis. Biochemical and Biophysical Research Communications, 519(2), 422–429. 10.1016/j.bbrc.2019.08.112 [PubMed: 31522816]

Palermo A, Strollo R, Maddaloni E, Tuccinardi D, D'Onofrio L, Briganti SI, … Napoli N (2015). Irisin is associated with osteoporotic fractures independently of bone mineral density, body composition or daily physical activity. Clinical Endocrinology, 82(4), 615–619. 10.1111/cen.12672 [PubMed: 25400208]

Park H-S, Kim HC, Zhang D, Yeom H, & Lim S-K (2018). The novel myokine irisin: Clinical implications and potential role as a biomarker for sarcopenia in postmenopausal women. Endocrine, 64, 341–348. 10.1007/s12020-018-1814-y [PubMed: 30570737]

Polyzos SA, Anastasilakis AD, Efstathiadou ZA, Makras P, Perakakis N, Kountouras J, & Mantzoros CS (2018). Irisin in metabolic diseases. Endocrine, 59(2), 260–274. 10.1007/s12020-017-1476-1 [PubMed: 29170905]

Qiao X, Nie Y, Ma Y, Chen Y, Cheng R, Yin W, … Xu L (2016). Irisin promotes osteoblast proliferation and differentiation via activating the MAP kinase signaling pathways. Scientific Reports, 6(1), 10.1038/srep18732

Qu X, Zhai Z, Liu X, Li H, Ouyang Z, Wu C, … Dai K (2014). Dioscin inhibits osteoclast differentiation and bone resorption though down-regulating the Akt signaling cascades. Biochemical and Biophysical Research Communications, 443(2), 658–665. 10.1016/j.bbrc.2013.12.029 [PubMed: 24333429]

Razidlo DF, Whitney TJ, Casper ME, McGee-Lawrence ME, Stensgard BA, Li X, … Westendorf JJ (2010). Histone deacetylase 3 depletion in osteo/chondroprogenitor cells decreases bone density and increases marrow fat. PLOS One, 5(7), e11492 10.1371/journal.pone.0011492 [PubMed: 20628553]

Rigueur D, & Lyons KM (2014). Whole-mount skeletal staining. Methods in Molecular Biology, 1130, 113–121. 10.1007/978-1-62703-989-5_9 [PubMed: 24482169]

Rodda SJ, & McMahon AP (2006). Distinct roles for Hedgehog and canonical Wnt signaling in specification, differentiation and maintenance of osteoblast progenitors. Development, 133(16), 3231–3244. 10.1242/dev.02480 [PubMed: 16854976]

Seeman E (2009). Bone modeling and remodeling. Critical Reviews in Eukaryotic Gene Expression, 19(3), 219–233. 10.1016/B978-0-12-416015-6.00004-6 [PubMed: 19883366]

Serbest S, Tiftikçi U, Tosun HB, & Kisa Ü (2017). The irisin hormone profile and expression in human bone tissue in the bone healing process in patients. Medical Science Monitor, 23, 4278–4283. 10.12659/MSM.906293 [PubMed: 28869754]

Sims NA, & Martin TJ (2014). Coupling the activities of bone formation and resorption: A multitude of signals within the basic multicellular unit. Bonekey Reports, 3, 10.1038/bonekey.2013.215

Singhal V, Lawson EA, Ackerman KE, Fazeli PK, Clarke H, Lee H, … Misra M (2014). Irisin levels are lower in young amenorrheic athletes compared with eumenorrheic athletes and non-athletes and are associated with bone density and strength estimates. PLOS One, 9(6), e100218 10.1371/journal.pone.0100218 [PubMed: 24926783]

Tang Y, Zhang L, Tu T, Li Y, Murray D, Tu Q, & Chen JJ (2018). microRNA-99a is a novel regulator of KDM6B-mediated osteogenic differentiation of BMSCs. Journal of Cellular and Molecular Medicine, 22(4), 2162–2176. 10.1111/jcmm.13490 [PubMed: 29377540]

Tsuchiya Y, Mizuno S, & Goto K (2018). Irisin response to downhill running exercise in humans. Journal of Exercise Nutrition & Biochemistry, 22(2), 12–17. 10.20463/jenb.2018.0011 [PubMed: 30149421]

Tu Q, Pi M, Karsenty G, Simpson L, Liu S, & Quarles LD (2003). Rescue of the skeletal phenotype in CasR-deficient mice by transfer onto the Gcm2 null background. Journal of Clinical Investigation, 111(7), 1029–1037. 10.1172/JCI17054 [PubMed: 12671052]

Varacallo MA, & Fox EJ (2014). Osteoporosis and its complications. Medical Clinics, 98(4), 817–831. 10.1016/j.mcna.2014.03.007 [PubMed: 24994054]

Wagner CL, & Greer FR (2008). Prevention of rickets and vitamin D deficiency in infants, children, and adolescents. Pediatrics, 122(5), 1142–1152. 10.1542/peds.2008-1862 [PubMed: 18977996]

Wang L, Mishina Y, & Liu F (2015). Osterix-Cre transgene causes craniofacial bone development defect. Calcified Tissue International, 96(2), 129–137. 10.1007/s00223-014-9945-5 [PubMed: 25550101]

Weischenfeldt J, & Porse B (2008). Bone marrow-derived macrophages (BMM): Isolation and applications. Cold Spring Harbor Protocols, 2008(12), pdb.prot5080 10.1101/pdb.prot5080 [PubMed: 21356739]

Wu LF, Zhu DC, Tang CH, Ge B, Shi J, Wang BH, … Lei SF (2018). Association of plasma irisin with bone mineral density in a large chinese population using an extreme sampling design. Calcified Tissue International, 103(3), 246–251. 10.1007/s00223-018-0415-3 [PubMed: 29582132]

Yan J, Liu H-J, Guo W-C, & Yang J (2018). Low serum concentrations of Irisin are associated with increased risk of hip fracture in Chinese older women. Joint, Bone, Spine, 85(3), 353–358. 10.1016/j.jbspin.2017.03.011 [PubMed: 28408276]

Zhai ZJ, Li HW, Liu GW, Qu XH, Tian B, Yan W, … Dai KR (2014). Andrographolide suppresses RANKL-induced osteoclastogenesis in vitro and prevents inflammatory bone loss in vivo. British Journal of Pharmacology, 171(3), 663–675. 10.1111/bph.12463 [PubMed: 24125472]

Zhang D, Bae C, Lee J, Lee J, Jin Z, Kang M, … Lim S-K (2018). The bone anabolic effects of irisin are through preferential stimulation of aerobic glycolysis. Bone, 114, 150–160. 10.1016/j.bone.2018.05.013 [PubMed: 29775761]

Zhang J, Valverde P, Zhu X, Murray D, Wu Y, Yu L, … Chen J (2017). Exercise-induced irisin in bone and systemic irisin administration reveal new regulatory mechanisms of bone metabolism. Bone Research, 5, 16056 10.1038/boneres.2016.56 [PubMed: 28944087]

Zhang L, Tang Y, Zhu X, Tu T, Sui L, Han Q, … Chen J (2017). Overexpression of miR-335-5p promotes bone formation and regeneration in mice. Journal of Bone and Mineral Research, 32(12), 2466–2475. 10.1002/jbmr.3230 [PubMed: 28846804]

Zhang M, Chen P, Chen S, Sun Q, Zeng Q-C, Chen J-Y, … Wang J-K (2014). The association of new inflammatory markers with type 2 diabetes mellitus and macrovascular complications: A preliminary study. European Review for Medical and Pharmacological Sciences, 18(11), 1567–1572. [PubMed: 24943964]

Zhou K, Qiao X, Cai Y, Li A, & Shan D (2019). Lower circulating irisin in middle-aged and older adults with osteoporosis: A systematic review and meta-analysis. Menopause, 10.1097/GME.0000000000001388

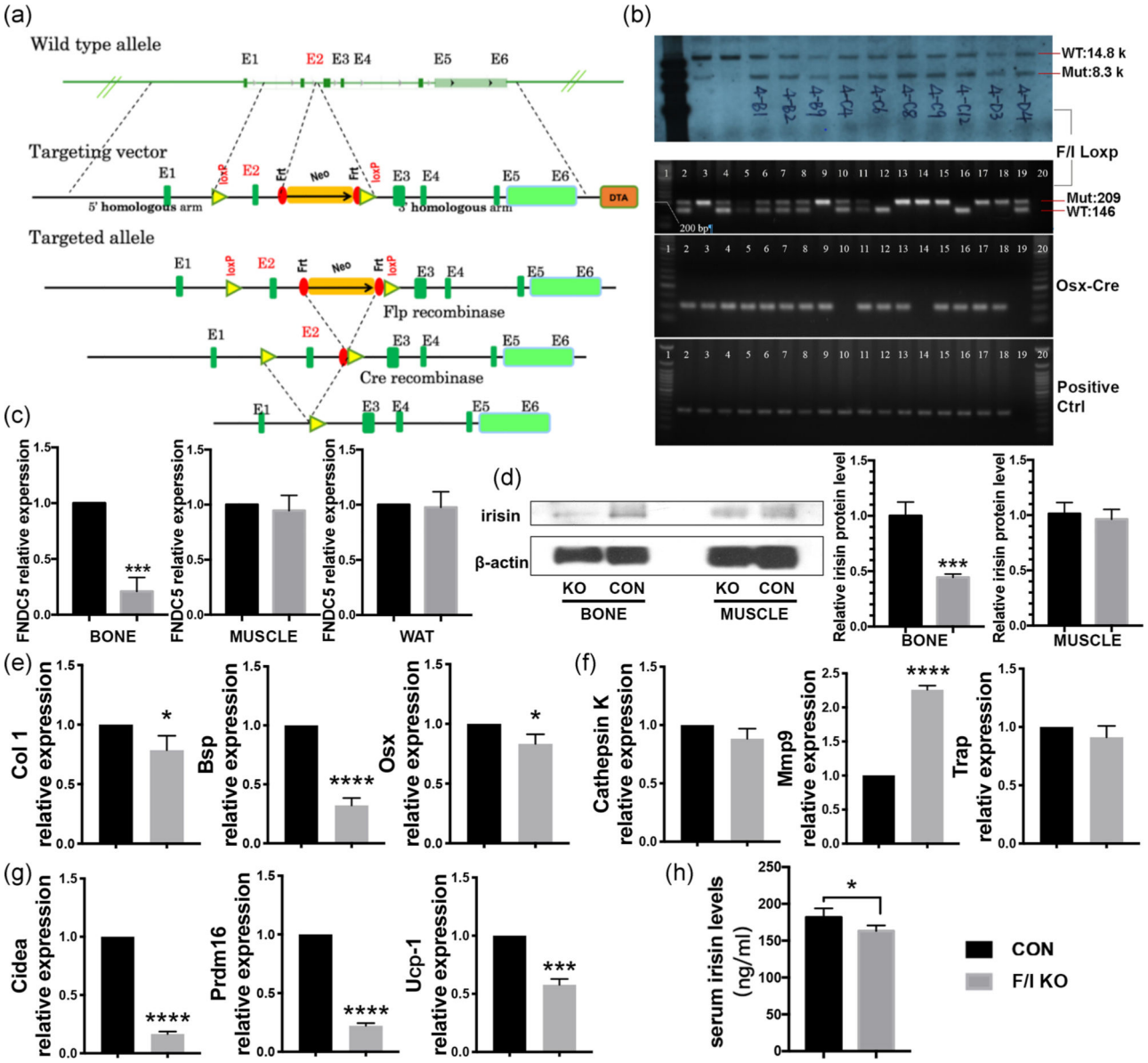

FIGURE 1.

Construction and identification of the F/I KO mice, and its implication in osteogenesis, browning effect and circulating irisin level in vivo. (a) The targeting strategy of FNDC5$^{flox/flox}$ mice. Truncated protein from deletion of exon2: MPPGPCAWPPRAALRLWLGCVCFALVQ AEEGCADAPVHSGGEHHHPVLRSLGPGGGHRIYRPCAGHLHPGTEPSQ* (28 aa N-terminal sequence of irisin and 47 aa frame-shifted nonsense aa). (b) Southern blot (upper) and standard PCR (lower) were performed to identify the FNDC5$^{flox/flox}$ ES cells and F/I KO mice. The FNDC5 mRNA expression level of bone, muscle and inguinal fat (c) and irisin protein level of bone and skeletal muscle (d) in F/I KO mice and control mice ($n = 3$). β-Actin was used as a loading control in western blot analysis. Relative mRNA level expression of osteogenic markers Col1, BSP, and OSX (e) and cathepsin K, Mmp9, and Trap

(f) in bone tissue (femur and tibia) of F/I KO and control mice were calculated and then normalized to GAPDH ($n = 3$). (g) The expression level of the genes related to white adipose tissue browning Cidea, Prdm16, and Ucp-1 in white adipose tissue (inguinal fat) of F/I KO and control mice ($n = 3$). (h) The circulating irisin level of F/I KO and control mice ($n = 6$). Values are shown as means ± *SD*. BSP, bone sialoprotein; Col1, collagen 1; CON, control; F/I KO, Osx-Cre:FNDC5/Irisin KO mice; GAPDH, glyceraldehyde 3-phosphate dehydrogenase; KO, knockout; Mmp9, matrix metalloproteinase 9; mRNA, messenger RNA; OSX, osterix; PCR, polymerase chain reaction; Prdm16, PR domain-containing 16; Trap, tartrate-resistant acid phosphatase; Ucp-1, uncoupling protein 1; WAT, white adipose tissue. *$p < .05$, ***$p < .001$, ****$p < .0001$ versus control

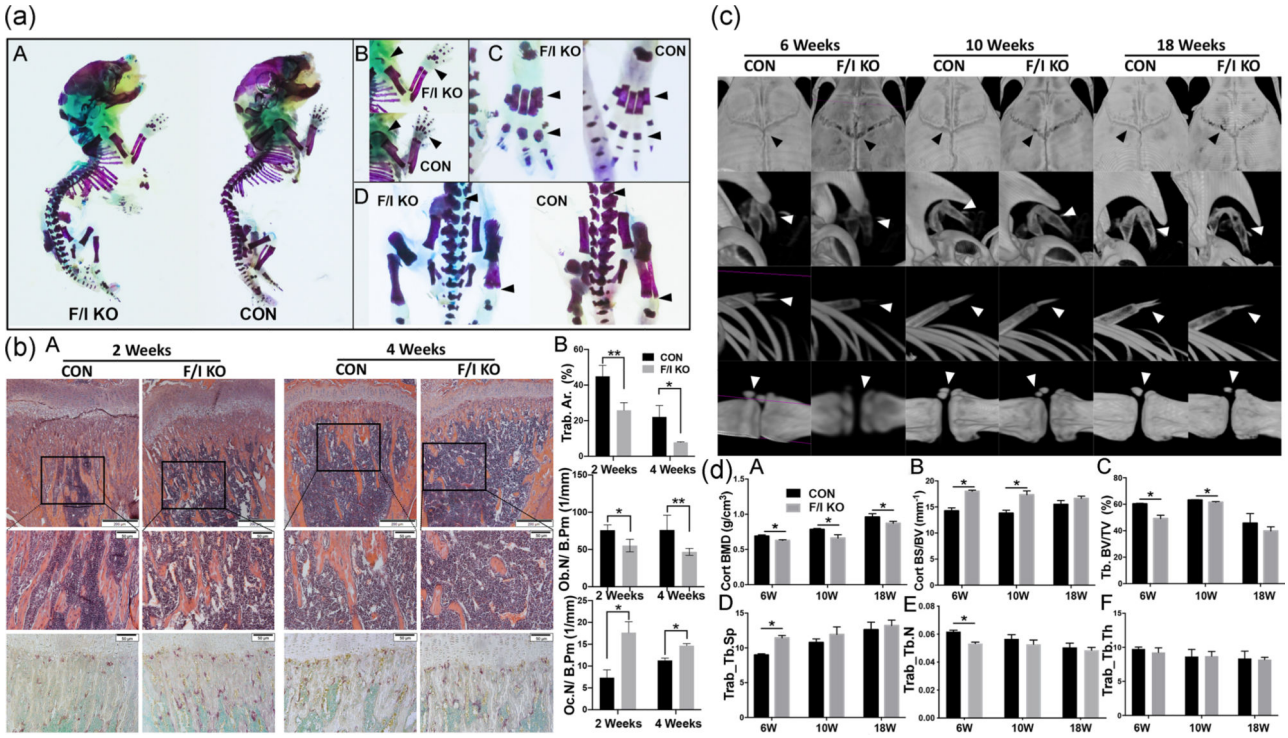

FIGURE 2.

Bone development and mineralization in F/I KO mice. (a) Cartilage matrix (blue) and mineralization (red) are showed by Alcian blue + alizarin red staining. (A) Whole mount staining of F/I KO mice (left) and control mice (right). Mineralization is decreased/delayed in the areas where Alcian blue staining is stronger in the KO mice. (B) The limb of F/I KO mice (above) and control mice (bottom). Mineralization is significantly decreased in the humerus and fingers (arrow). (C) Feet of F/I KO mice (left) and control mice (right). The toe bone of F/I KO mice are less mature than the control (arrow). (D) Lumbar of F/I KO mice (left) and control mice (right). Alcian blue staining showed more cartilage matrix in the KO group (arrow). (b) Bone histology and histomorphometry. (A) H&E staining of longitudinal sections of the femur (upper; ×4 magnification; scale bar = 200 μm). H&E (middle) and TRAP staining (lower) of primary ossification centers (×20 magnification; scale bar = 50 μm). (B) Histomorphometric quantification of Tb.Ar%, Ob.N/B.Pm, and Oc.N/B.Pm. (c) Representative three-dimensional model reconstructions of live animal μCT scan data shows the mineralization of the skull (first row), hyoid (second row), ribs and xiphoid (third row) and coccyx (last row) of the F/I KO mice and control mice at 6, 10, and 18 weeks. (d) Cort. BMD (A), Cort. BS/BV (B), Trab. BV/TV (C), Tb.Sp (D), Tb.N (E), and Tb.Th (F) in femurs of knockout and control mice at 6, 10 and 18 weeks ($n = 5$). Values are shown as means ± *SD*. CON, control; Cort.BMD, cortical bone mineral density; Cort.BS/BV, cortical bone surface/bone volume; F/I KO, Osx-Cre:FNDC5/Irisin KO mice; H&E, hemotoxylin and eosin; KO, knockout; Ob.N/B.Pm, osteoblast number per bone perimeter; Oc.N/B.Pm, osteoclast number per bone perimeter; Tb.Ar%, trabecular bone area; Tb.N, trabecular number; Tb.Sp, trabecular separation; Tb.Th, trabecular thickness; Trab.BV/TV, trabecular bone volume/tissue volume; Trap, tartrate-resistant acid phosphatase; μCT, microcomputed tomography. *$p < .05$ versus control

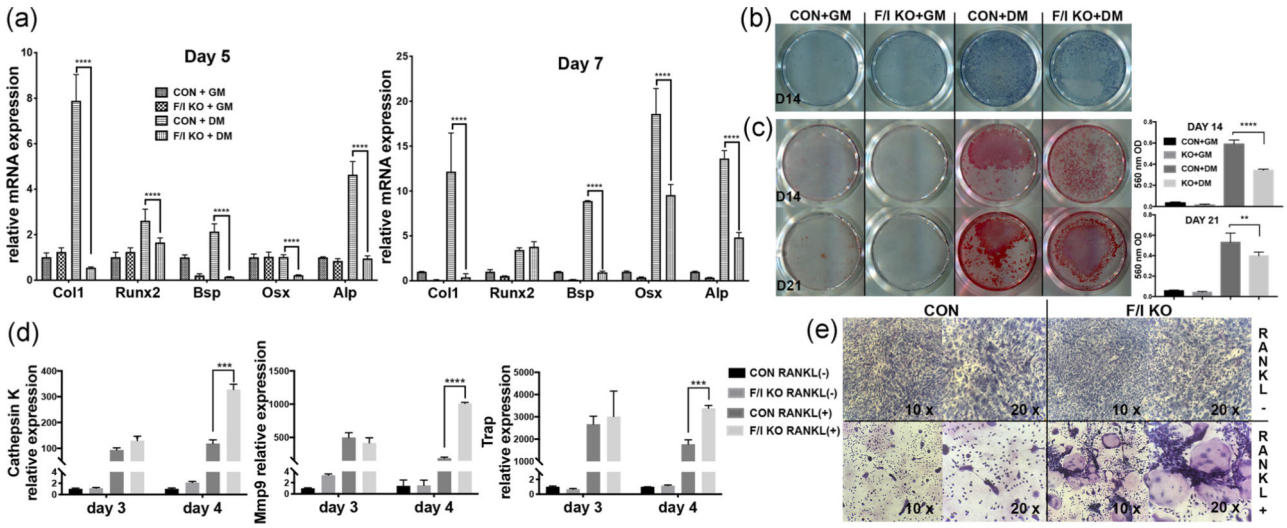

FIGURE 3.

Characterization of FNDC5/irisin deficiency BMSCs and BMMs isolated and cultured in vitro. (a) The mRNA expression of osteogenic markers on Day 5 and Day 7 ($n = 3$). The BMSCs were treated with either growth medium (GM) or osteoblast differentiation medium (DM) including ascorbic acid (Asc, 50 μg/ml), dexamethasone (Dex, 0.1 μM) and β-glycerophosphate (β-Gly, 10 mM) in the presence or absence of irisin. (b) ALP staining of BMSCs from F/I KO and control mice after treated with or without osteogenic supplements for 14 days. (c) Pictures of ARS staining and concentration of melted nodules solution on Day 14 (upper lane) and Day 21 (lower lane). (d) The mRNA expression level of cathepsin K, Mmp9, and Trap in RANKL-induced osteoclast culture on Day 3 and Day 4 ($n = 3$). (e) TRAP staining of BMMs from F/I KO and control mice in the presence or absence of RANKL for 4 days. Values are shown as means ± *SD*. ALP, alkaline phosphatase; ARS, alizarin red S; Asc, ascorbic acid; BMM, bone marrow–derived macrophage; BMSC, bone marrow–derived mesenchymal cell; CON, control; Dex, dexamethasone; DM, differentiation medium; F/I KO, Osx-Cre:FNDC5/irisin KO mice; FNDC5, fibronectin-type III domain-containing 5; GM, growth medium; KO, knockout; Mmp9, matrix metalloproteinase 9; mRNA, messenger RNA; RANKL, receptor activator of nuclear factor-κB ligand; TRAP, tartrate-resistant acid phosphatase; β-Gly, β-glycerophosphate. $^{**}p < .01$, $^{***}p < .001$, $^{****}p < .0001$ versus control

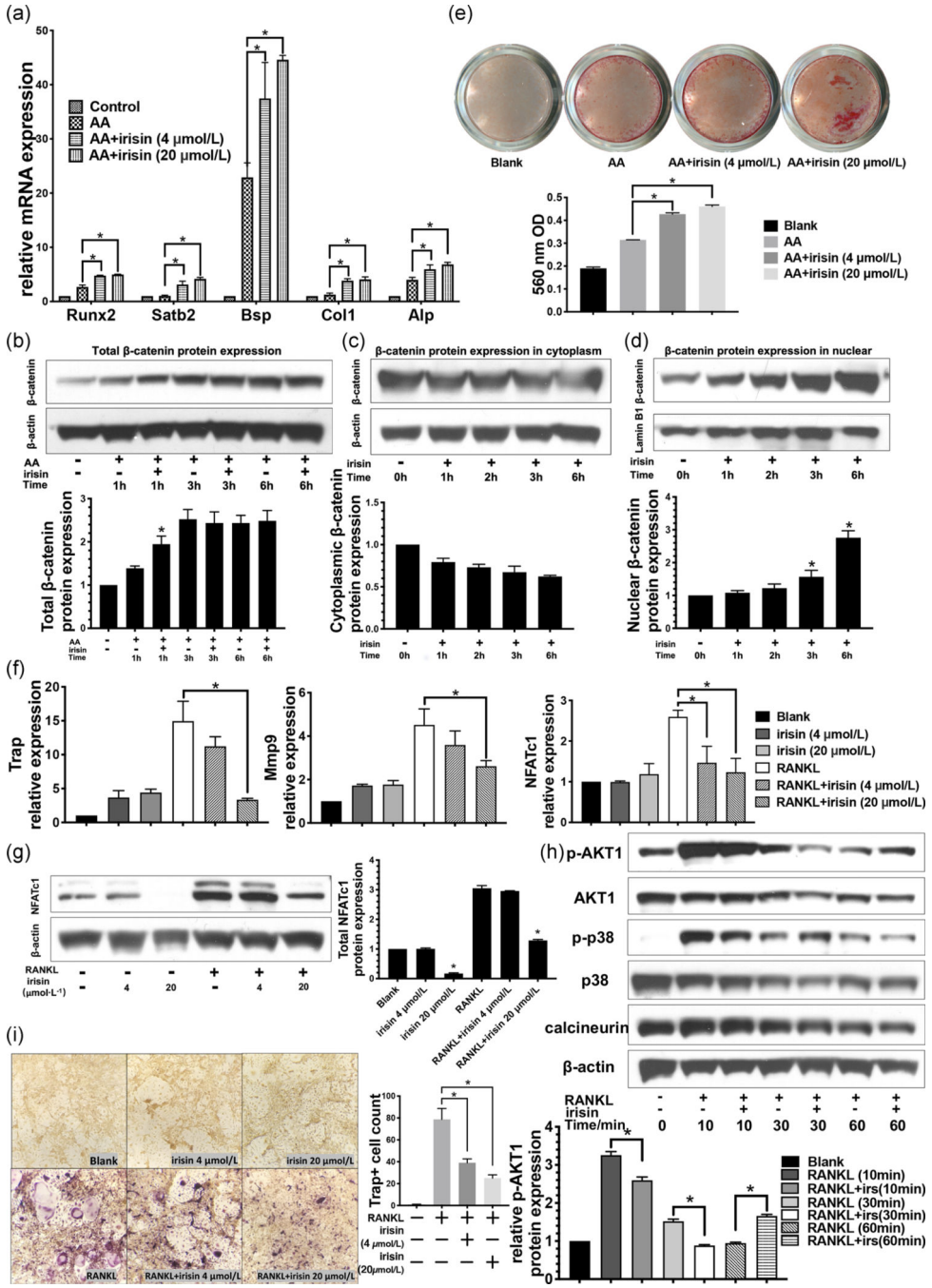

FIGURE 4.

The effects of r-irisin on osteoblast and osteoclast differentiation in BMSCs and BMMs. (a) Real-timePCR analysis of the mRNA expression level of osteogenic related gene markers on Day 5 ($n = 3$). (b) Total protein level of β-catenin in BMSCs during the osteoblast-induced cell culture with or without r-irisin. (upper lane). β-Actin was used as a loading control (lower lane; $n = 3$). The β-catenin protein level in cytoplasmic (c) and nuclear (d) fractions and the relative expression calculated using β-actin or lamin B1 as loading controls for cytoplasmic and nuclear expression, respectively ($n = 3$). (e) Alizarin red staining for bone

nodules of osteoblast-induced BMSCs culture with and without irisin for 3 weeks. (f) The mRNA expression level of osteoclastogenesis gene expression on Day 5 ($n = 3$). (g) Nfatc1 protein expression on Day 5. (h) Western blot analyses with antibodies recognizing p-Akt1, Akt1, p-p38, p38, and calcineurin in osteoclast-induced BMMs treated with and without irisin. β-Actin was used as a loading control. (i) TRAP staining and quantitative analysis of the $TRAP^+$ MNCs. All values are shown as mean ± *SD*. AA, amino acid; Alp, alkaline phosphatase; BMM, bone marrow–derived macrophage; BMSC, bone marrow–derived mesenchymal cell; BSP, bone sialoprotein; Col1, collagen 1; CON, control; F/I KO, Osx-Cre:FNDC5/irisin KO mice; KO, knockout; MNC, multinucleated cell; mRNA, messenger RNA; Nfatc1, nuclear factor of activated T cells c1; PCR, polymerase chain reaction; RANKL, receptor activator of nuclear factor-κB ligand; Runx2, Runt-related transcription factor 2; TRAP, tartrate-resistant acid phosphatase. *$p < .05$ versus control

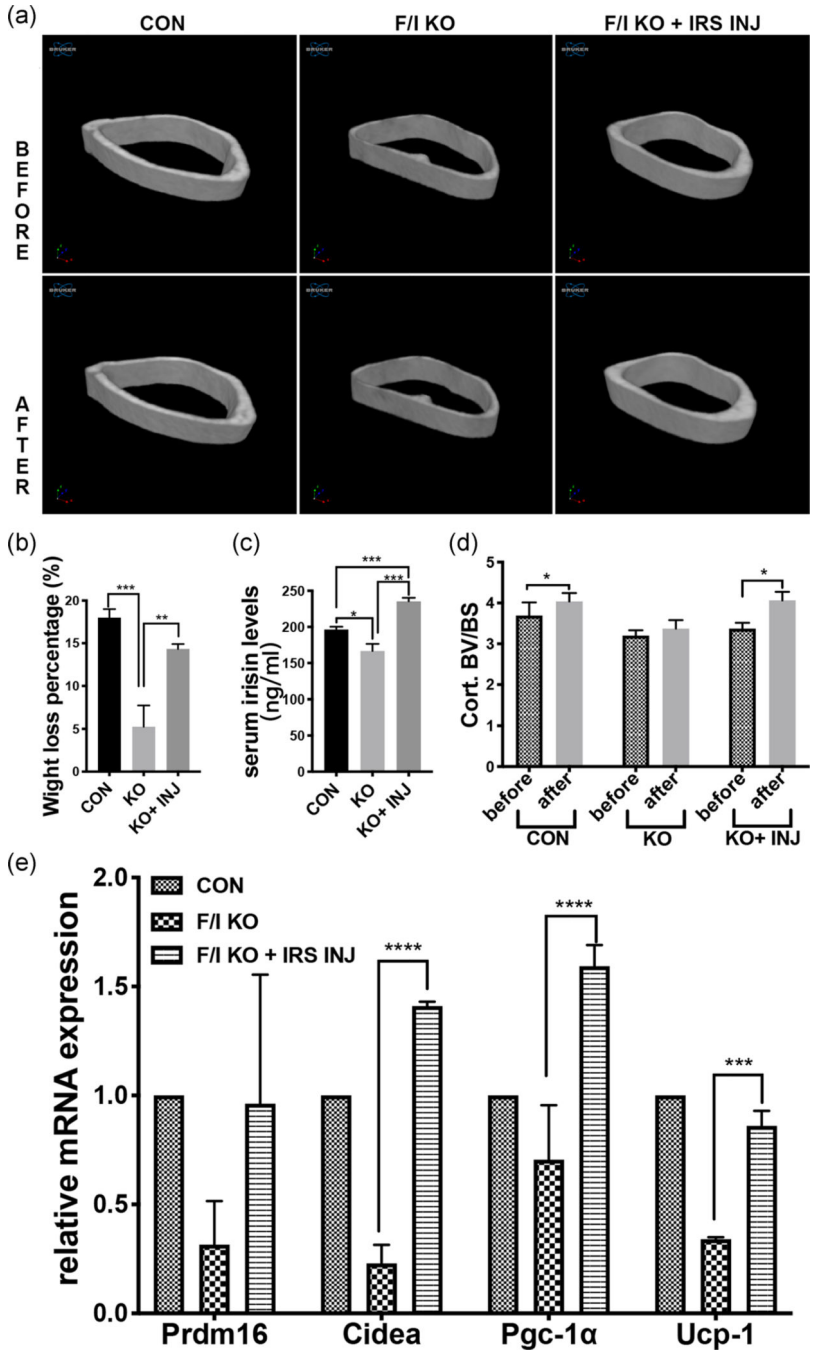

FIGURE 5.

Changes after wheel running and daily irisin injection for 14 days. (a) Micro-CT 3D reconstruction of cortical bone (right femur), before and after. (b) The body weight loss percentage of control, F/I KO and F/I KO with the irisin injection group were 18 ± 0.58, 5.25 ± 1.25, and 14.3 ± 0.33, respectively ($n = 5$). (c) Serum irisin level after wheel running and injection for 14 days ($n = 5$). (d) Cort.BV/BS of the three groups before and after the exercise and injection. (e) Relative mRNA expression level of the genes related to white adipose tissue browning Cidea, Prdm16, Pgc-1α and Ucp-1 in white adipose tissue (inguinal

fat) before and after the exercise and injection ($n = 5$). Values are shown as mean ± *SD*. CON, control; Cort.BV/BS, cortical bone surface/bone volume; F/I KO, Osx-Cre:FNDC5/irisin KO mice; IRS INJ, irisin injection; KO, knockout; mRNA, messenger RNA; Pgc-1α, peroxisome proliferator-activated receptor-γ coactivator 1α; Prdm16, PR domain-containing 16; Ucp-1, uncoupling protein 1. *$p < .05$, ***$p < .001$, ****$p < .0001$ versus control